*Desalination and Water Treatment*
www.deswater.com

1944-3994/1944-3986 © 2012 Desalination Publications. All rights reserved
doi: 10.1080/19443994.2012.672203

43 (2012) 63–75
April

# The feasibility of using *Rosa canina* galls as an effective new biosorbent for removal of methylene blue and crystal violet

Esra Bağda

*Chemistry Department, Faculty of Science, Cumhuriyet University, Sivas 58140, Turkey*
*Tel. +90 346 2191010-2991; Fax: +90 346 2191186; email: esraer@cumhuriyet.edu.tr*

Received 9 March 2011; Accepted 12 February 2012

## ABSTRACT

In this study, removal of two cationic dyes, basic blue 9 (BB9) and basic violet 3 (BV3) with *Rosa canina* galls (RCG), was investigated. The parameters that affect the biosorption process such as pH of the solution, amount of biosorbent and initial dye concentration were studied. The kinetic and thermodynamic parameters of biosorption were calculated with batch systems. The optimum pH for the adsorption system was 5.0 and 7.0 for BB9 and BV3, respectively. The adsorption process followed the Freundlich model and pseudo-second-order kinetics. The maximum adsorption capacities were 107.53 $\mathrm{mg\,g^{-1}}$ and 312.50 $\mathrm{mg\,g^{-1}}$ for BB9 and BV3, respectively. The thermodynamic study indicated that the adsorptions of these cationic dyes were spontaneous and endothermic. The results show that RCG has a potential as an effective low-cost biosorbent for removal of cationic dyes.

*Keywords: Rosa canina* gall; Biosorption; Dye removal

## 1. Introduction

Water pollution arising from dyeing industry effluents is an important ecological problem because these effluents contain significant amount of coloured organic substances. Untreated disposal of this coloured water into aquatic mediums like rivers causes damage to aquatic life or to human beings by their mutagenic and carcinogenic effect [1]. Even small quantities of dyes can colour large water bodies, resulting in reduction of penetration of light and photosynthetic activity. So, the coloured organic substances have to be removed properly before they are discharged into the water resources [2].

For removal or degradation of contaminants, several methods including biological and physico-chemical technologies have been developed such as anaerobic treatment, coagulation, electrocoagulation, flotation, filtration, ion exchange, membrane separation, oxidation and advanced oxidation [3–11]. However, most of those methods have suffered from some of the disadvantages such as inefficient removal of dye, relatively high operating cost and high-energy requirement [12,13]. Adsorption technique is quite simple, and there is a wide range of adsorbents available [14–17]. Therefore, in the past few years, scientists focused on the idea of developing cheaper and "useless" materials as adsorbent [18–28]. These useless materials called biosorbents have been proposed as promising alternatives to activated carbon. Biosorbents are materials of biological origin which are used for removal of organic or inorganic species [29]. Some biomaterials including fungi, algae, agricultural by-products or residues have been explored as new low-cost sorbents [12].

Plant galls are abnormal growths of plant cells formed as a response to the insect's stimulus caused by egg laying, or larvae or nymphs feeding. The ability to form galls represents an important and widespread life style among insects. They can be found on roots, stems, leaves, flowers and seeds. The galls are formed around the developing larva some time after the adult female has laid the egg on a carefully selected part of a particular plant and development to an adult insect is completed within the gall. Most of the galls are harmless and just look interesting. On the other hand, certain species can physically and aesthetically damage high value plants by reducing photosynthesis and seed production, discolouring foliage, causing defoliation, branch dieback and rarely, plant death [30,31].

According to Coruh and Ercisli [32], RCG which is caused by an insect, *Diplolepis* sp., is an important problem and so common in all rose-growing areas in Turkey. The insect lays its eggs on flower buds of rose canina and induces RCG on the seeds and developed RCG causes with or without split open rose fruits. Severe gall formation causes fruit deformations. The insect reduces fruit yields and fruit quality and affected fruit are not marketable, owing to the presence of the galls [32].

In this study, RCG were used as low-cost biosorbents for removing two cationic dyes (basic blue 9 [BB9] and basic violet 3 [BV3]) from the aqueous solution. These dyes have been chosen as model molecules for industrial dyes. The effect of initial pH, contact time, initial dye concentration, amount of RCG and temperature was studied to explain batch adsorption process of the dyes on RCG. Thermodynamic and kinetic parameters were also studied to elucidate the adsorption of the dyes on to RCG samples.

## 2. Materials and methods

### *2.1. Preparation of biosorbent (RCG) and chemicals*

RCG were collected from the Karacalar region of UlaŞ, Sivas. The raw material was first washed with distilled water to separate crude dust and dried for about two days at room temperature. The samples were crushed, washed with distilled water and dried at 353 K; the excess moisture was removed at 373 K in about 1 h. The dry material was sieved to obtain particle sizes: <53 μm, 53–150 μm, 150–300 μm and 300–600 μm with an Octagon 200 model equipment. The size > 600 μm was not studied. The samples were stored in a closed bottle.

BB9 is a thiazin (methylene blue, CI: 52015, FW: 373.91 g mol$^{-1}$), BV3 is a triphenylmethane (crystal violet, CI: 42555, FW: 407.98 g mol$^{-1}$), they were purchased from Sigma-Aldrich Ltd., Germany and used without further purification. Solutions used for pH adjustment were prepared from HCl and NaOH purchased from Merck, Darmstadt, Germany. All the solutions were prepared in distilled water.

### *2.2. Characterization of the biosorbent*

#### *2.2.1. Point of zero charge*

Point of zero charge of RCG was determined by the solid addition method [33]. RCG (0.1 g) was added to 12 vials containing solutions of different initial $pH_0$ (1–12), which were also adjusted with 0.1 M sodium hydroxide or hydrochloric acid. The whole system was shaken for 24 h at room temperature. The final pH ($pH_f$) of solutions was measured with a Sartorius basic model pH meter, with a glass electrode. The ΔpH value was calculated from the difference between initial and final pH and plotted against the initial pH. The value of pH corresponds to $\Delta pH = 0$ which was taken as point of zero charge.

#### *2.2.2. Surface acidity and basicity of RCG*

Surface acidic and basic properties of RCG were determined using the method given by Brito et al. [33]. For surface acidity, 0.01 g RCG samples were shaken in 50 mL of 0.01 M of NaOH for 24 h and then filtered off. The remaining NaOH was back-titrated potentiometrically with 0.01 M of HCl.

For surface basicity, 0.01 g RCG samples were shaken in 50 mL of 0.01 M of HCl for 24 h, and then filtered and the remaining HCl was back-titrated potentiometrically with 0.01 M of NaOH.

#### *2.2.3. Surface morphology characterization, BET surface area and pore volume of RCG*

The surface morphology of RCG was examined using JEOL/JSM-6335F model scanning electron microscopy (SEM). Multipoint BET surface area and pore volume analysis was done with Quantachrome NOVA 4000 E model analyser. Before BET surface area analysis, RCG sample was dried at 373 K for about 6 h and degassed under nitrogen atmosphere at 383 K for about 5 h.

### *2.3. Adsorption studies and parameters that affect the adsorption of dyes*

For adsorption studies predetermined volume of dye solution at desired pH, and RCG were shaken with a Nüve S 350 model multi-shaker for predetermined contact time. Effect of temperature studies was carried out with Nüve ST 402 multi-shaker-water bath system. The spectrophotometric measurements were recorded with a Shimadzu UV 1800 model spectrophotometer, with a quartz cell. Absorbance values were measured at 665 nm for BB9 and 591 nm for BV3. All absorbance values were recorded after separation of RCG particles via filter paper, so calibration solutions were also filtered to eliminate the effect of loss of dye during filtration. To eliminate the effect of any contribution to absorbance because of soluble materials released from RCG sample, absorbance values were taken against blank solution (without dye) prepared with same amount of RCG.

The amount of dye biosorbed per gram of RCG at any time, $Q_t$, was calculated as follows:

$$Q_t = \frac{V(C_0 - C_t)}{m} \tag{1}$$

where $V$ is the volume of solution (L), $C_0$ and $C_t$ are the initial and instant (respectively) concentration of dye (mg/L) and $m$ is the mass of biosorbent (g).

Efficiency (or degree) of dyes removal (%), at any time, was calculated as follows:

$$\text{Removal } \% = 100\frac{C_0 - C_t}{C_0} \tag{2}$$

#### 2.3.1. Effect of solution pH on adsorption

The effects of pH on adsorption of BB9 and BV3 were studied in the range of pH 2.1–9.1 and 2.1–9.0, respectively, using 50 mL of 24 mg/L of dye solution. The pH of the dye solution was adjusted with 0.1 M NaOH and HCl. The same procedure was applied for the investigation of effect of pH for BV3.

#### 2.3.2. Effect of particle size on adsorption

The effects of particle size on the adsorption of dyes were studied for four fractions: <53 µm, 53–150 µm, 150–300 µm, 300–600 µm. The pH of dye solutions were adjusted to 5.0 and 7.0 for BB9 and BV3, respectively. Fifty millilitres of 24 mg/L dye solutions was contacted with 0.05 g of RCG with different particle sizes for 3 h.

#### 2.3.3. The effect of temperature on adsorption

The effects of temperature on adsorption of dyes on RCG were studied in a similar way with the effect of pH, with the same volume of solutions, initial dye concentrations and amount of RCG. The pH of dye solutions were adjusted to 5.0 and 7.0 for BB9 and BV3, respectively. Only the temperature of suspension was changed and was studied in the range of 298–328 K.

#### 2.3.4. The effect of RCG dose

The effect of RCG dose was investigated by contacting different amount of biosorbent (0.01–0.07 g) with 100 mL of 24 mg/L of each dye solution individually.

### 2.4. Desorption studies

Desorptions of BB9 and BV3 were performed according to Fernandez et al. [34]. RCG samples (1.0 g) were loaded with 24 mg/L of each dye solution individually for 3 h. The RCG samples were separated and washed with distilled water to remove excess dye. The samples were dried at 333 K for 24 h. Dry materials (0.05 g) were contacted with 50 mL of three different eluting solvents: distilled water, 0.1 M of HCl and 0.01 M of $CH_3COOH$. Desorption percentages were calculated from the Eq. (3):

$$\text{Desorption of dye}\% = 100 \times \frac{\text{mass release (mg)}}{\text{mass initially biosorbed (mg)}} \tag{3}$$

## 3. Results and discussion

### 3.1. Characterization of the biosorbent

Point of zero charge for a given surface is the pH at which surface has a neutral charge [35,36]. Point of zero charge, $pH_{pzc}$, was determined as 4.7 (figure is not shown), at lower pH ($pH < 4.7$) surface of RCG is positively charged, at higher pH ($pH > 4.7$) surface of RCG is negatively charged, so the adsorption of cationic dye becomes favourable when $pH > 4.7$. The biosorption of BB9 and BV3 was carried out at $pH > 4.7$ (5.0 for BB9 and 7.0 for BV3).

Surface acidic and basic properties of RCG were determined with a back-titration method described in Section 2.2.2. and the result was 0.70 mmol/g $OH^-$ and 0.98 mmol/g $H^+$.

The textual structure of RCG can be observed from the SEM photograph (Fig. 1). The SEM images show porous and irregular surface morphology.

According to multipoint BET analysis, the surface area of RCG is 0.376 $m^2/g \pm 5\%$ and pore volume is 0.002 $cm^3/g$ (Fig. 2, Table 1). The high values of adsorption capacities of RCG in spite of surface area are due to the high content of tannins [32]. The polyhydroxy polyphenol groups of tannin are though the active sides in the adsorption process.

### 3.2. Effect of solution pH on adsorption

The pH may be the one of the most important parameters that affects the adsorption of the dyes on

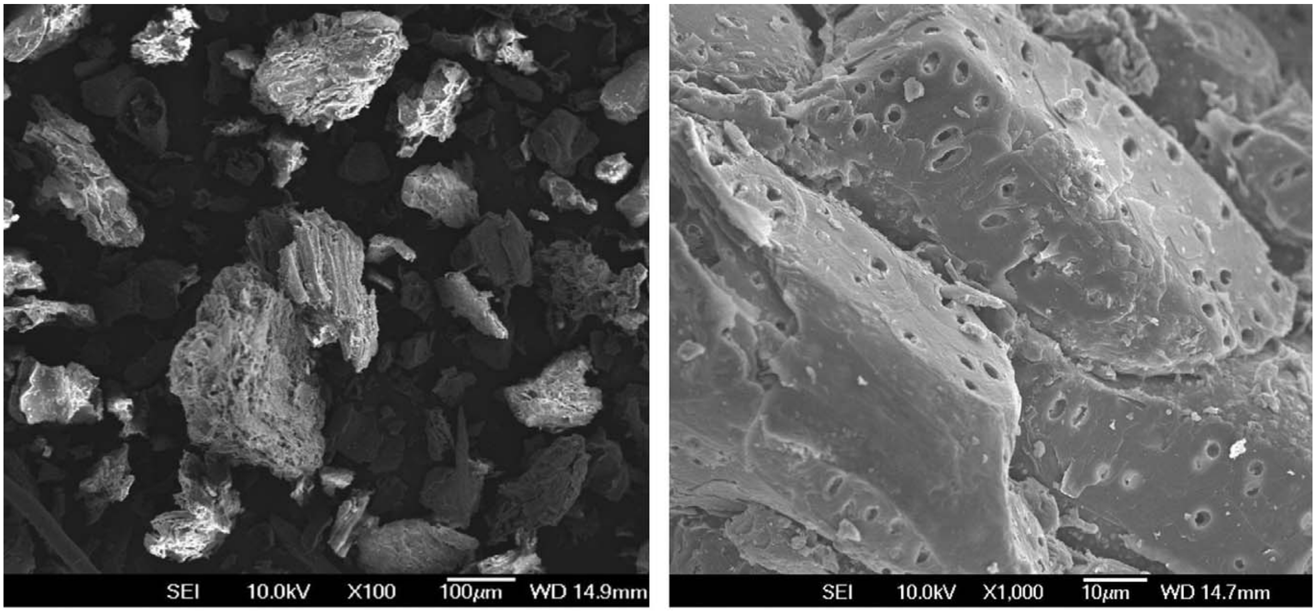

(a) (b)

Fig. 1. SEM photograph for RCG (a) 100-fold and (b) 1,000-fold magnification.

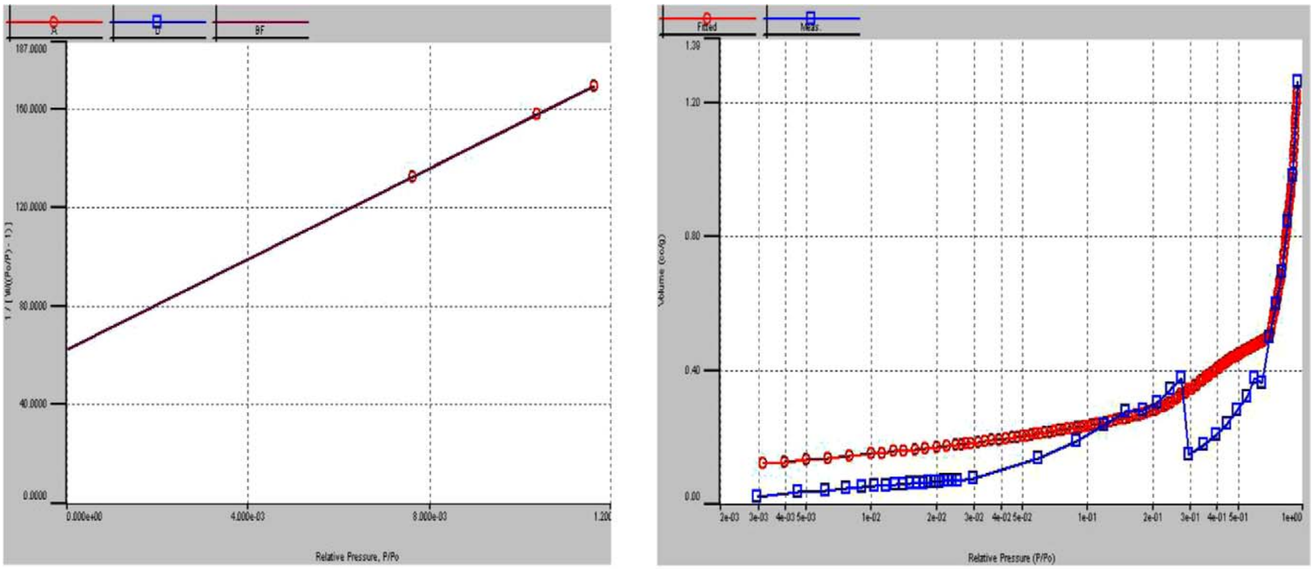

(a) (b)

Fig. 2. (a) Multi-point BET plot and (b) DFT fitting comparison of RCG.

an active surface. Generally, the interaction between dye molecules and RCG is basically a combined result of charges on dye molecules and the surface of sorbent. The effect of solution pH was studied keeping the dye concentration and amount of RCG fixed and varying the pH: 2.1–9.1. Changing the pH of the solution from acidic region to basic region, the surface of biosorbent becomes more negatively charged, resulting in enhancing the adsorption of cationic dyes. The effect of pH on the adsorption of BB9 and BV3 on RCG is shown in Fig. 3. Greater uptake for the dyes at higher pH is due to the electrostatic attraction between the negatively charged sites of RCG and the positively charged cationic dye molecules. In addition, increasing solution pH will increase the number of hydroxyl groups, which will thereby increase the

Table 1
BET summary, DFT method summary, surface area data, pore volume data, pore size data of RCG

| BET[1] summary | | DFT[2] method summary | |
|---|---|---|---|
| Slope | 9202.998 | Pore volume | 0.002 cc/g |
| Intercept | 6.257e+01 | Lower confidence limit | 0.003 μ |
| Correlation coefficient | 0.999964 | Fitting error | 5.318% |
| C constant | 148.083 | Pore width (mode) = | 0.004 μ |
| Surface area | 0.376 m/g | Moving point average | Off |

| | |
|---|---|
| *Surface area data* | |
| Multipoint BET | 3.759e−01 m$^2$/g |
| Langmuir surface area | 6.570e+00 m$^2$/g |
| BJH[3] method cumulative adsorption surface area | 3.059e+00 m$^2$/g |
| BJH method cumulative desorption surface area | 1.092e+00 m$^2$/g |
| DH[4] method cumulative adsorption surface area | 3.345e+00 m$^2$/g |
| DH method cumulative desorption surface area | 1.143e+00 m$^2$/g |
| DR[5] method micropore area | 2.686e+00 m$^2$/g |
| NLDFT[6] cumulative surface area | 8.293e−01 m$^2$/g |
| *Pore volume data* | |
| Total pore volume for pores with Diameter less than 0.24 μ at P/Po = 0.991878 | 3.054e−03 cc/g |
| BJH method cumulative adsorption pore volume | 3.765e−03 cc/g |
| BJH method cumulative desorption pore volume | 3.381e−03 cc/g |
| DH method cumulative adsorption pore volume | 3.756e−03 cc/g |
| DH method cumulative desorption pore volume | 3.331e−03 cc/g |
| DR method micropore volume | 9.547e−04 cc/g |
| HK[7] method cumulative pore volume | 9.596e−04 cc/g |
| NLDFT method cumulative pore volume | 1.867e−03 cc/g |
| *Pore size data* | |
| Average pore diameter | 3.250e−02 μ |
| BJH method adsorption pore diameter | 1.585e−03 μ |
| BJH method desorption pore diameter | 6.469e−03 μ |
| DH method adsorption pore diameter | 1.585e−03 μ |
| DH method desorption pore diameter | 6.469e−03 μ |
| DR method micropore pore width | 5.566e−03 μ |
| DA[8] method pore diameter | 2.700e−03 μ |
| HK method pore diameter | 5.315e−04 μ |
| SF[9] method pore diameter | 1.200e−03 μ |
| NLDFT pore diameter | 3.537e−03 μ |

Notes: [1]BET: Branauer–Emmet–Teller method, [2]DFT: Density Functional Theory Method, [3]BJH Barrett–Joyner–Halenda method, [4]DH: Dollimore Heal method, [5]DR: Dubinn–Radushkevic method (DR), [6]NLDFT: nonlocal density functional theory, [7]HK: Horvath–Kawazoe Method, [8]DA: Dubinin–Astakhov method, [9]SF: Saito-Foley method (DA), cc/g: cm$^3$/g.

number of negatively charged sites and will strengthen the attraction between dye molecules and the RCG surface. It has been found that the adsorption of dyes increases with increase in pH and maximum adsorption is found 5.0 for BB9 and 7.0 for BV3. At higher pH, the repulsion between the biosorbent surface and the partial negative charge due to chloride ion on both dyes causes A slight decrease in biosorption of the dyes [14].

As the biomass will have a net positive charge at pH values below the point of zero charge (pH < 4.7), biosorption of cationic dyes will be reduced due to the change in the overall surface charge on the RCG. Moreover at lower pH values,

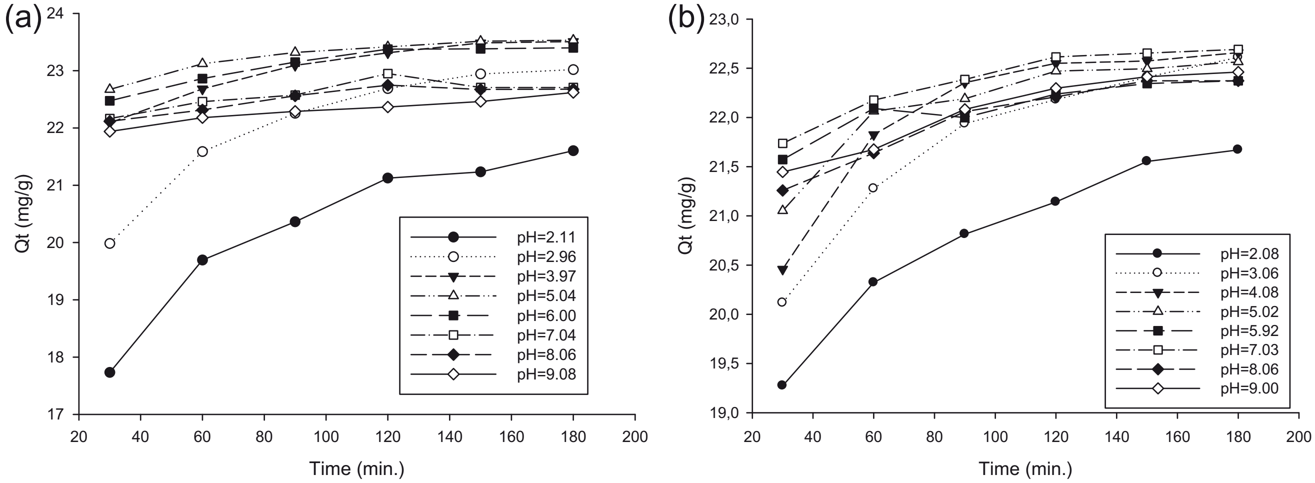

Fig. 3. Effect of pH on uptake of (a) BB9 and (b) BV3, $C_0 = 24.0$ mg/L, at 298 K.

the availability of negatively charged RCG surface sites will be reduced due to the presence of excess $H^+$ ions competing with cationic dye molecules for adsorption sites.

### 3.3. Effect of particle size

Fig. 4 shows the influence of particle size on biosorption. With decrease in particle size of the RCG, the adsorbed amount of dyes increases due to increase in their surface area and the availability of more adsorption sites. No significant change was observed for particle size < 300 µm. Also, adsorption rate increases as the particle size decreases for both dyes because diffusion of dye molecules to the adsorption site is easy for smaller particles, so time elapsed to reach equilibrium for adsorption process is less than 30 min for particles < 150 µm.

### 3.4. Effect of temperature and adsorption thermodynamics

The effects of temperature on adsorption of dyes were studied in the range of 298.15–328.15 K. Fig. 5 shows the effect of temperature for BB9 and BV3, respectively. The amount of adsorbed dyes increased with increase of temperature, as expected for an endothermic adsorption process.

The thermodynamic studies were carried out at 298.15, 308.15, 318.15 and 328.15 K using 50 mL of 24 mg/L dye solution and 0.05 g of RCG biosorbent. The thermodynamic parameters, Gibbs free energy ($\Delta G^0$), enthalpy ($\Delta H^0$), entropy ($\Delta S^0$) and the

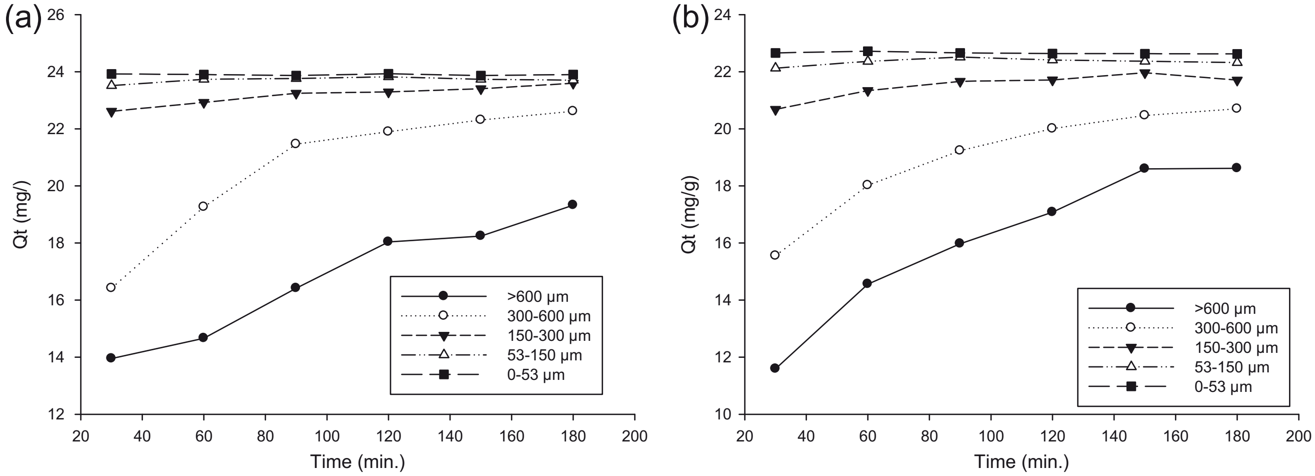

Fig. 4. Influence of particle size on uptake of (a) BB9, pH = 5.0 and (b) BV3 pH = 7.0, $C_0 = 24.0$ mg/L, at 298 K.

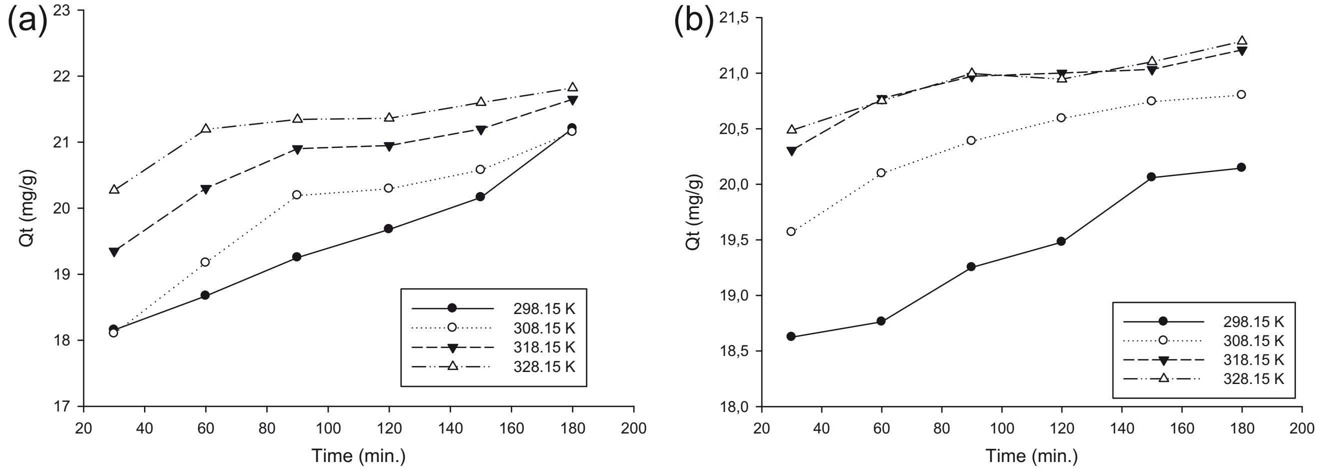

Fig. 5. Influence of temperature on uptake of (a) BB9, pH = 5.0 and (b) BV3 pH = 7.0, $C_0 = 24.0$ mg/L.

equilibrium constant ($K_c$), were calculated from Eqs. (4) and (5) [33]:

$$\log K_c = -\frac{\Delta H^0}{2.303RT} + \frac{\Delta S^0}{2.303R} \tag{4}$$

$$K_c = \frac{C_{ads}}{C_e} \tag{5}$$

where $C_e$ and $C_{ads}$ (mg/L) are the equilibrium and adsorbed concentrations and $R$ is the universal gas constant (8.314 J/mol K).

The biosorption enthalpy and entropy values were calculated from the slope and intercept of the linear plot of log $K_c$ vs. $1/T$ plot. Using Eq. (6):

$$\Delta G = -2.303RTlog(K_c) \tag{6}$$

The thermodynamic parameters, Gibbs free energy ($\Delta G^0$), enthalpy ($\Delta H^0$), entropy ($\Delta S^0$) and the equilibrium constant ($K_c$), are presented in Tables 2 and 3 for BB9 and BV3. The negative values of $\Delta G^0$ and the positive values of $\Delta H^0$ indicate that the biosorption of dyes on RCG was spontaneous and endothermic [37]. The endothermic adsorption has also been reported for the adsorption of Direct red 28 onto activated carbon prepared from coir pith, an agricultural solid waste [38]. Normally, adsorption is an exothermic process for especially gases. For the adsorption from solutions solubility factor superimposed the normal temperature effect. If the solubility of adsorbate increases with increase in temperature, the adsorption decreases. On the other hand, if the solubility of adsorbate decreases with increase in temperature, then the normal temperature effect and the solubility effect will work against each other and the adsorption may show an increase or a decrease depending on which parameter is predominant [39].

### 3.5. The effect of biosorbent dose

Fig. 6 shows the influence of biosorbent dose on the adsorption of BB9 and BV3 on to RCG. The percentage of adsorbed dye increased up to 0.04 g of RCG, due to availability of more adsorption sites. On account of the fact that almost all dye molecules adsorbed to active sites before 0.04 g of RCG, no significant change was observed above 0.04 g of RCG.

### 3.6. Desorption studies

To explain the mechanisms of biosorption and the possibility of recovery of both dyes and the biosor-

Table 2
Thermodynamic parameters of BB9

| $T$ (K) | $K_c$ | $\Delta H^0$ (kJ mol$^{-1}$) | $\Delta S^0$ (J mol$^{-1}$ K$^{-1}$) | $R^2$ | $\Delta G^0$ (kJ mol$^{-1}$) | Dye removal (%) |
|---|---|---|---|---|---|---|
| 298.15 | 7.589 | 8.43 | 44.75 | 0.92 | −5.02 | 88.35 |
| 308.15 | 7.42 | | | | −5.14 | 88.12 |
| 318.15 | 9.21 | | | | −5.87 | 90.21 |
| 328.15 | 10.00 | | | | −6.28 | 90.91 |

Table 3
Thermodynamic parameters of BV3

| $T$ (K) | $K_c$ | $\Delta H^0$ (kJ mol$^{-1}$) | $\Delta S^0$ (J mol$^{-1}$ K$^{-1}$) | $R^2$ | $\Delta G^0$ (kJ mol$^{-1}$) | Dye removal (%) |
|---|---|---|---|---|---|---|
| 298.15 | 5.23 | 11.26 | 51.84 | 0.93 | −4.10 | 83.94 |
| 308.15 | 6.50 | | | | −4.80 | 86.67 |
| 318.15 | 7.60 | | | | −5.37 | 88.37 |
| 328.15 | 7.84 | | | | −5.62 | 88.69 |

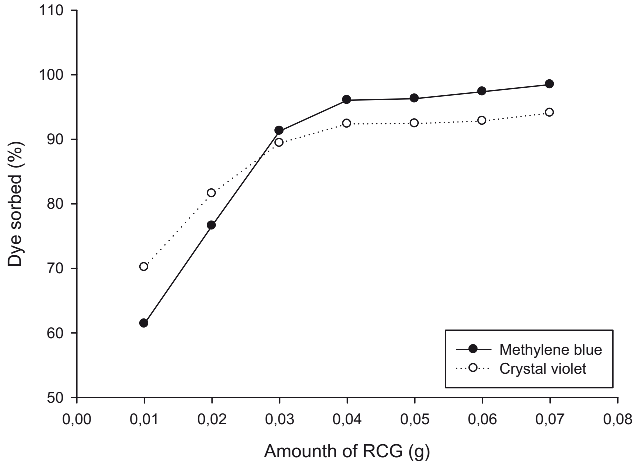

Fig. 6. Effect of biosorbent dose on uptake of BB9, pH = 5.0 and BV3 pH = 7.0, $C_0$ = 24.0 mg/L, at 298 K.

bent, desorption experiments were performed by a batch process at room temperature. The percentage recovery results are summarised in Table 4.

The reversibility of adsorption strongly depends on the characteristic of binding. Strong binding forces such as covalent bonding result in chemical adsorption and weak binding forces such as Van der waals forces result in physical adsorption. Chemical adsorption is difficult to reverse. The desorption studies show that adsorbed dyes could not be desorbed significantly by using water, dilute solutions of acetic acid and hydrochloric acid. The maximum desorption percentages were 7.17 for BB9 and 11.83 for BV3 and these percentages were achieved with 0.1 M of $CH_3COOH$. The low desorption of the dyes indicates the formation of some chemical bonds between biosorbent and dyes [34,40] and dyes might have been chemisorbed onto the surface of the biosorbent [38].

Table 4
Desorption percentage of BB9 and BV3 with different eluents

| Dye | Eluent | Desorption of dyes (%) |
|---|---|---|
| BB9 | Water | 1.02 |
| | $CH_3COOH$ | 7.17 |
| | HCl | 5.87 |
| BV3 | Water | 5.90 |
| | $CH_3COOH$ | 11.83 |
| | HCl | 4.60 |

### 3.7. Kinetics of biosorption process

The adsorptions of BB9 and BV3 were investigated as a function of time to elucidate the time to reach equilibrium. Plots of $Q_t$ vs. $t$ are shown in Fig. 7 for different initial concentrations. The figure indicates that the amount of adsorbed dye ($Q_t$) increases with the increase of initial concentration of both dyes. The process is almost complete at 40 mins for initial concentration of < 28 mg/L for both dyes. The adsorption rates of dyes were rapid at initial stages of the process, then these values reached equilibrium in less than 100 min for BB9 and 80 min for BV3, for especially an initial dye concentration higher than 28 mg/L. Rapid removal of dyes caused by the diffusion and adsorption of dyes to macro pores of RCG surface, the slow removal was caused by diffusion of micro pores [37]. The other reason is that, when the exterior surface of RCG reached saturation, the dye molecules entered into interior pores. This accounts for the fact that the second process takes a relatively long time [2].

The intraparticle diffusion rate was studied using the Eq. (7) [33,41]

$$Q_t = K_{id}\sqrt{t} + C \tag{7}$$

where $Q_t$ is the amount of dye adsorbed at time $t$, $K_{id}$ is the intraparticle rate constant and C is the intercept. A plot of $Q_t$ vs. $t^{1/2}$ has a slope equal to $K_{id}$, and intercept equal to C. If C≠0, the intraparticle diffusion is not the only rate control step but also other processes may control the rate of adsorption. Fig. 8 shows that $Q_t$ vs. $t^{1/2}$ plot does not cross the origin and has two linear sections with different slopes (Table 5), so intraparticle diffusion shows a multistep manner in nature: the diffusion to macropores and diffusion into micropores [41].

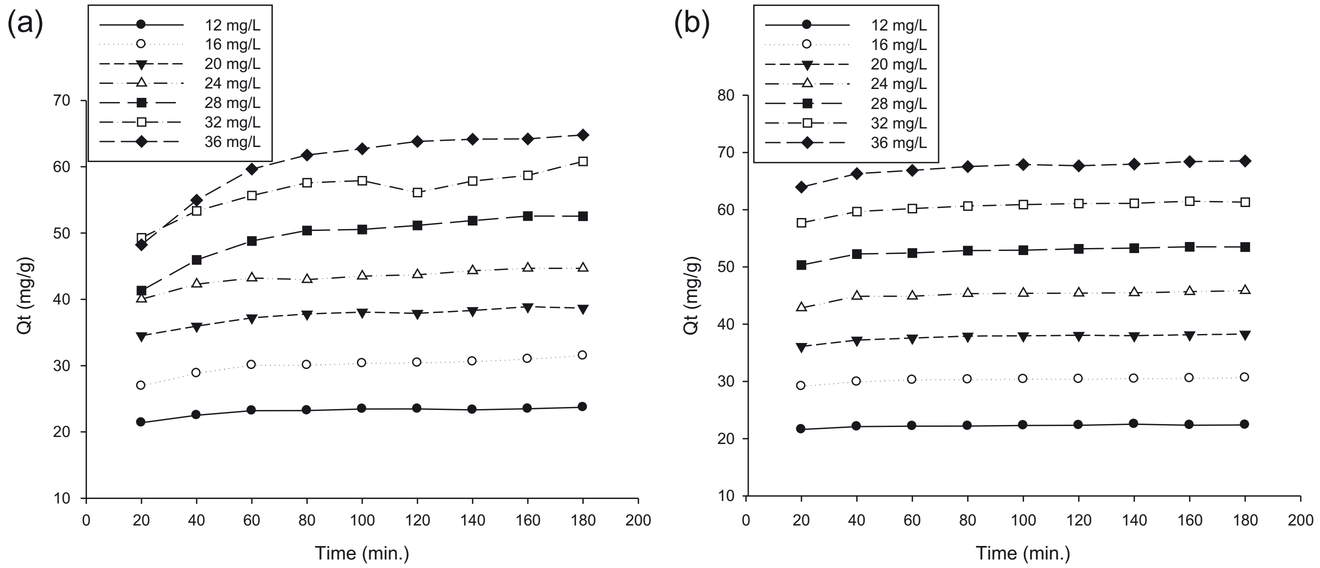

Fig. 7. Effect of contact time on uptake of (a) BB9, pH = 5.0 and (b) BV3 pH = 7.0, at 298 K.

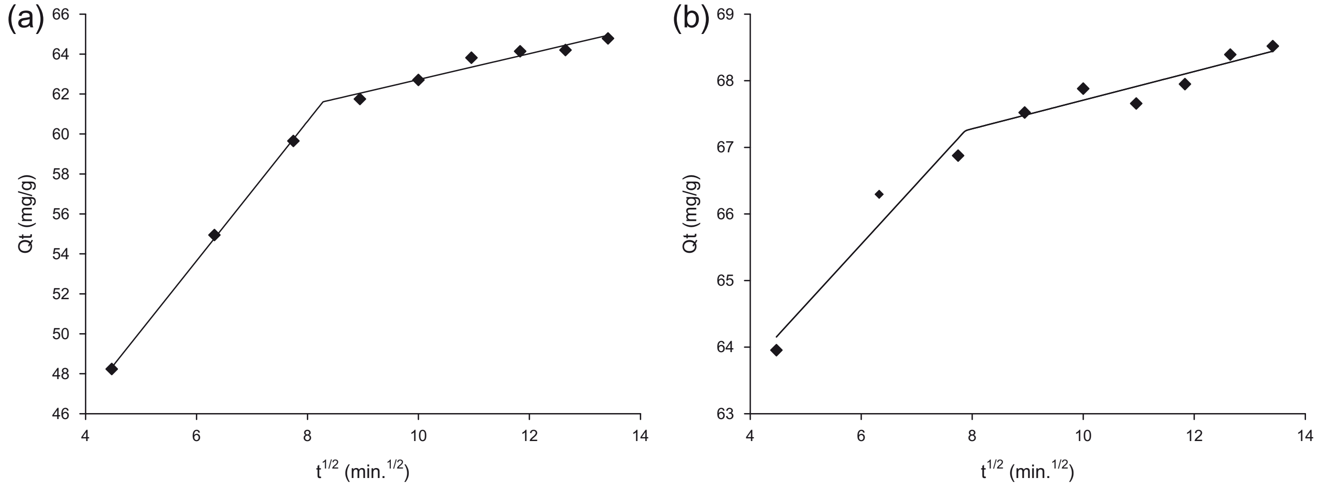

Fig. 8. Intraparticle diffusion plots for (a) BB9, pH = 5.0 and (b) BV3 pH = 7.0. at initial concentration of 36 mg/L, and at 298 K.

Table 5
Intraparticle diffusion rate constants

| BB9 | | | | BV3 | | | |
|---|---|---|---|---|---|---|---|
| $k_{i,1}$ | $R^2$ | $k_{i,2}$ | $R^2$ | $k_{i,1}$ | $R^2$ | $k_{i,2}$ | $R^2$ |
| 3.49 | 0.99 | 0.65 | 0.93 | 0.91 | 0.93 | 0.22 | 0.82 |

### 3.7.1. The first-order kinetic model

Kinetic data of dyes were treated with Lagergren first-order rate equation. This model is a widely used adsorption rate equation for the adsorption of solute from a liquid solution. Lagergren first-order equation is given by [33,41]:

$$\frac{dQ_t}{dt} = k_1(Q_e - Q_t) \tag{8}$$

Integrating Eq. (8) for the boundary conditions $t = 0$ to $t = t$, $Q = 0$ to $Q = Q_t$, the equation becomes:

$$\ln(Q_e - Q_t) = \ln Q_e - k_1 t \tag{9}$$

where $Q_t$ and $Q_e$ (mg/g) are the amounts of dye adsorbed at equilibrium and time $t$, $k_1$ is the rate constant of pseudo-first-order adsorption. $k_1$ and $\ln Q_e$ values were calculated from the slope and intercept of the linear plot of $\ln(Q_e - Q_t)$ vs. $t$.

The rate constant of pseudo-first-order adsorption and $Q_e$ are presented in Table 6.

#### 3.7.2. The Second-order kinetic model

The kinetic data of dyes were also treated with second-order rate equation proposed by Ho et al. [37,41]:

$$\frac{dQt}{dt} = k_2(Q_e - Q_t)^2 \tag{10}$$

Rearranging Eq. (10) and using the boundary conditions $t = 0$ to $t = t$, $Q = 0$ to $Q = Q_t$, the equation becomes:

$$\frac{t}{Q_t} = \frac{1}{\mathrm{k}_2 Q_e^2} + \frac{t}{Q_e} \tag{11}$$

where $Q_t$ and $Q_e$ (mg/g) are the amounts of dye adsorbed at equilibrium and time $t$, $k_2$ is the pseudo-second-order rate constant. $k_2$ and $Q_e$ values were calculated from the slope and intercept of the linear plot of $t/Q_t$ vs. $t$. The rate constant of pseudo-second-order adsorption and $Q_e$ are presented in Table 6.

High correlation coefficients showed that data of adsorption process in this study strictly fit the pseudo-second-order rate kinetic model rather than pseudo-first order kinetic model. $h$ is the initial adsorption rate; the expression is given by [41]

$$h = k_2 Q_e^2 \tag{12}$$

### 3.8. Adsorption isotherms

Adsorption isotherm equations explain the relations between the equilibrium concentrations and uptake up to equilibrium. Adsorption isotherms are generally used to explain the performance of the systems. Two types of isotherms within the literature, the Langmuir and the Freundlich, are widely used for elucidating the adsorption behaviour of dyes from aqueous solutions. Constants of isotherms depend on some characteristics of the sorbent, like surface properties. Adsorption isotherms are generally used to compare the capacities of different sorbents [14].

The Langmuir equation is given as

$$Q_e \frac{Q_e K C_e}{1 + KC_e} \tag{13}$$

where $Q_e$ is the amount of dye per mass of biosorbent ($\mathrm{mg\,g^{-1}}$), $Q_{max}$ is the monolayer capacity ($\mathrm{mg\,g^{-1}}$), $C_e$ is the equilibrium concentration ($\mathrm{mg\,L^{-1}}$) and $K$ is a constant that is related to the energy of adsorption. Although Langmuir isotherm has been developed for gas phase adsorption, this equation can also be useful for liquid phase adsorption [42]. The Langmuir equation is valid for monolayer sorption onto a completely homogeneous surface (identical sites with the same adsorption energy), it assumes that the interaction between adsorbed molecules is negligible [43–45]. Once a reactive molecule occupies a site, no further adsorption can take place at the same site [46]. A linear expression of the Langmuir equation is given by

$$\frac{C_e}{Q_e} = \frac{C_e}{Q_{max}} + \frac{1}{KQ_{max}} \tag{14}$$

A plot of $C_e/Q_e$ vs. $C_e$ is a line with a slope equal to $1/Q_{max}$ and intercept equal to $1/(KQ_{max})$.

Table 6
Pseudo-first- and second-order rate parameters for BB9, pH = 5.0 and BV3, pH = 7.0, at 298 K

| Dye | Pseudo-first-order rate parameters | | | | Pseudo-second-order rate parameters | | | | |
|---|---|---|---|---|---|---|---|---|---|
| | $C_0$ (mg/L) | $Q_e$ | $k_1$ | $R^2$ | $C_0$ (mg/L) | $Q_e$ | $k_2$ | $h$ | $R^2$ |
| BB9 | 36.0 | 21.98 | 0.021 | 0.98 | 36.0 | 68.03 | $1.76 \times 10^{-3}$ | 8.12 | 0.99 |
| | 24.0 | 5.87 | 0.019 | 0.88 | 24.0 | 45.46 | $6.45 \times 10^{-3}$ | 13.33 | 0.99 |
| BV3 | 36.0 | 4.95 | 0.011 | 0.92 | 36.0 | 68.97 | $3.88 \times 10^{-3}$ | 38.02 | 0.99 |
| | 24.0 | 2.72 | 0.010 | 0.87 | 24.0 | 46.08 | $1.47 \times 10^{-2}$ | 31.15 | 0.99 |

The Freundlich isotherm equation is given as below

$$Q_e = K_f C_e^{1/n} \tag{15}$$

where $Q_e$ is the amount adsorbed per mass of adsorbent, $K_f$ is the Freundlich constant, $C_e$ is the equilibrium concentration and $n$ is the heterogeneity factor [33,47]. Freundlich model is generally better suited for the multilayer adsorption process compared to the Langmuir model [44].

A linear form of the Freundlich isotherm can be written as

$$\ln Q_e = \ln K_f + \frac{1}{n} \ln C_e \tag{16}$$

A plot of ln $Q_e$ vs. ln $C_e$ is a line with a slope equal to $1/n$ and intercept equal to ln $K_f$ [48].

The results of experimental data over the investigated concentration range are summarized in Table 7. The applicability of Langmuir and Freundlich models was established from the regression correlation and fitted curves. It is obvious from $r^2$ values on the table that, adsorption data of BB9 and BV3 best fit the Freundlich isotherm model. $Q_{max}$ values are also shown in Table 7; these results suggest that 1 g of RCG adsorbs more BV3 than BB9. The Freundlich constant $n$ is an empirical parameter that varies with the level of heterogeneity indicating the degree of nonlinearity between dye uptake capacity and unadsorbed dye concentration and is related to the distribution of bonded ions on the sorbent surface. The $n$, Freundlich constant, should have values lying in the range of 1–10 for classification as favourable adsorption [47,49,50]. In general, $n > 1$ illustrates that adsorbate is favourably adsorbed on an adsorbent and the higher the $n$ value, the stronger the adsorption intensity. For this study, $n$ is significantly higher than unity, 2.12 for BB9, 1.50 for BV3, both dye ions are favourably adsorbed by RCG. As more detailed, according to Tseng and Wu [49], BB9 having a $1/n$ value (0.472) in the range of $0.1 < 1/n < 0.5$ indicates the favourable adsorption and BV3 (0.665) in the range of $0.5 < 1/n < 1$ indicates the pseudo-linear adsorption characteristic.

### 3.9. Biosorption mechanism

Biosorption mechanism may be influenced by some factors such as weak and strong interactions, steric hindrances, surface properties, pH of solution,

Table 7
Langmuir and Freundlich parameters for BB9 and BV3

| Dye | Langmuir parameters | | | Freundlich parameters | | |
|---|---|---|---|---|---|---|
| | $Q_{max}$ (mg/g) | $K$ (L/mg) | $R^2$ | $K_f$ (L/mg) | $n$ | $R^2$ |
| BB9 | 107.53 | 1.02 | 0.99 | 51.32 | 2.12 | 0.99 |
| BV3 | 312.50 | 0.21 | 0.92 | 49.45 | 1.50 | 0.98 |

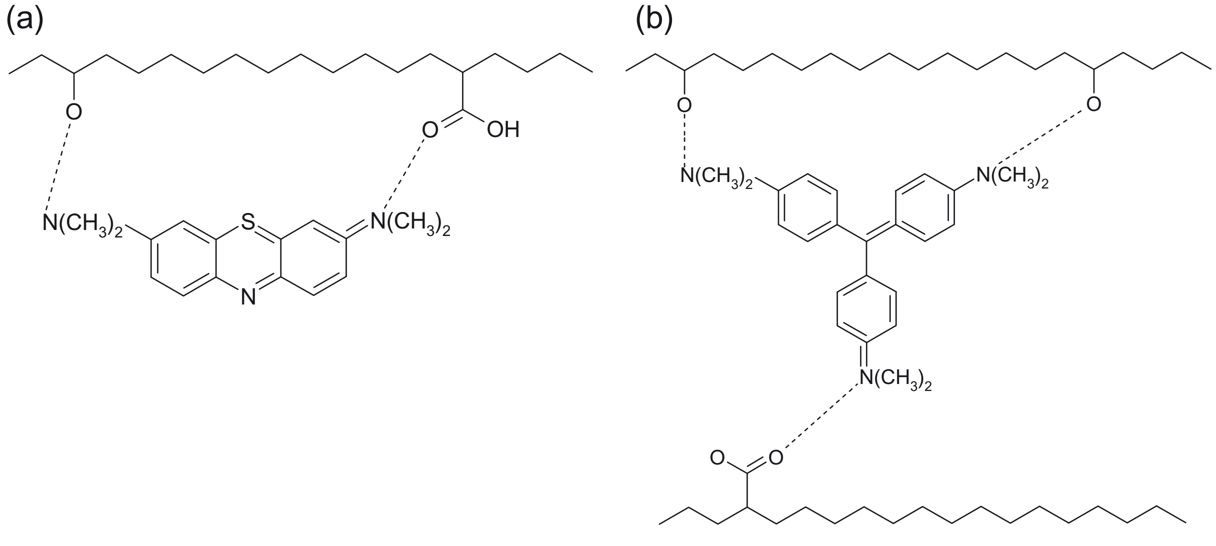

Fig. 9. Biosorption mechanism of (a) BB9 and (b) BV3.

etc. BB9 and BV3 are cationic dyes and they have partial positive charge on nitrogen atoms (two amino groups for BB9 and three for BV3) (Fig. 9). The strong interactions may occur due to electrostatic interaction and hydrogen bonding between dye molecules (amino groups) and RCG surface (partial negative sides).

### 4. Conclusion

Adsorptions of two cationic dye, BB9 and BV3, on RCG, inexpensive and useless biomaterial were studied in batch mode. The 88% of BB9, 84% of BV3 were removed successfully. The adsorption data followed the Freundlich model with satisfactory maximum adsorption capacities, 107.53 mg/g and 312.50 mg/g for BB9 and crystal blue, respectively. The negative values of Gibbs free energy indicated the spontaneity of adsorption process. Finally, this study confirmed that RCG is an alternative effective biosorbent for removal of BB9 and BV3. The RCG is abundantly available in Turkey and hence its application for the removal of dyeing effluents is expected to be economically feasible. It may also be useful in the treatment of other especially organic effluents.

## References

[1] T. Santhi, S. Manonmani, T. Smitha, Removal of malachite green from aqueous solution by activated carbon prepared from the epicarp of *Ricinus communis* by adsorption, J. Hazard. Mater. 179 (2010) 178–186.

[2] R. Kumar, R. Ahmad, Biosorption of hazardous crystal violet dye from aqueous solution onto treated ginger waste (TGW), Desalination 265 (2010) 112–118.

[3] A. Hussain, T. Parveen, P. Kumar, I. Mehrotra, Phenolic wastewater: Effect of F/M on anaerobic degradation, Desalin. Water Treat. 2 (2009) 254–259.

[4] E. Khelifi, H. Bouallagui, Y. Touhami, J.J. Godon, M. Hamdi, Enhancement of textile wastewater decolourization and biodegradation by isolated bacterial and fungal strains, Desalin. Water Treat. 2 (2009) 310–316.

[5] S. Shanmugama, P. Rajasekaran, J.V. Thanikal, Synthetic dye decolourization, textile dye and paper industrial effluent treatment using white rot fungi Lentines edodes, Desalin. Water Treat. 4 (2009) 143–147.

[6] F. Banat, S. Al-Asheh, R. Zomaout, B. Qtaishat, T. Alateat, S. Almayta, Photodegradation of methylene blue dye using bentonite as a catalyst, Desalin. Water Treat. 5 (2009) 283–289.

[7] N. Zaghbani, A. Hafiane, M. Dhahbi, Removal of Direct Blue 71 from wastewater using micellar enhanced ultrafiltration, Desalin. Water Treat. 6 (2009) 204–210.

[8] H. Jirankova, J. Mrazek, P. Dolecek, J. Cakl, Organic dye removal by combined adsorption–membrane separation process, Desalin. Water Treat. 20 (2010) 96–101.

[9] M. Sarioglu, T. Bisgin, Decolorization of Basic Red 46 and Methylene Blue by anaerobic sludge: Biotic and abiotic processes, Desalin. Water Treat. 23 (2010) 61–65.

[10] G. Yuzhu Fu, T. Viraraghavan, Removal of Disperse Red 1 from an aqueous solution by fungus *Aspergillus niger*, Desalin. Water Treat. 25 (2011) 187–194.

[11] B.H. Hameed, U.G. Akpan, K.P. Wee, Photocatalytic degradation of Acid Red 1 dye using ZnO catalyst in the presence and absence of silver, Desalin. Water Treat. 27 (2011) 204–209.

[12] B.C. Oei, S. Ibrahim, S. Wang, H.M. Ang, Surfactant modified barley straw for removal of acid and reactive dyes from aqueous solution, Bioresour. Technol. 100 (2009) 4292–4295.

[13] B.E. TaŞtan, S. Ertuğrul, G. Dönmez, Effective bioremoval of reactive dye and heavy metals by *Aspergillus versicolor*, Bioresour. Technol. 101 (2010) 870–876.

[14] P. Sharma, R. Kaur, C. Baskar, W.J. Chung, Removal of methylene blue from aqueous waste using rice husk and rice husk ash, Desalination 259 (2010) 249–257.

[15] A.S. Franca, L.S. Oliveira, A.A. Nunes, C.C.O. Alves, Microwave assisted thermal treatment of defective coffee beans press cake for the production of adsorbents, Bioresour. Technol. 101 (2010) 1068–1074.

[16] T. Jesionowski, Characterization of pigments obtained by adsorption of C.I. Basic Blue 9 and C.I. Acid Orange 52 dyes onto silica particles precipitated via the emulsion route, Dyes Pigments 67 (2005) 81–92.

[17] T. Jesionowski, A. Andrzejewska, A. Krysztafkiewicz, Adsorption of basic dyes from model aqueous solutions onto novel spherical silica support, Color. Technol. 124 (2008) 165–172.

[18] H. Aydin, G. Baysal, Y. Bulut, Utilization of walnut shells (*Juglans regia*) as an adsorbent for the removal of acid dyes, Desalin. Water Treat. 2 (2009) 139–147.

[19] R. Han, W. Zou, Y. Li, X. Liu, M. Tang, Equilibrium, kinetic and mechanism study for the adsorption of neural red onto rice husk, Desalin. Water Treat. 12 (2009) 210–218.

[20] A.S. Franca, L.S. Oliveira, S.A. Saldanha, P.I.A. Santos, S.S. Salum, Malachite green adsorption by mango (*Mangifera indica* L.) seed husks: Kinetic, equilibrium and thermodynamic studies, Desalin. Water Treat. 19 (2010) 241–248.

[21] O. Hamdaoui, F. Saoudi, M. Chiha, Utilization of an agricultural waste material, melon (*Cucumis melo* L.) peel, as a sorbent for the removal of cadmium from aqueous phase, Desalin. Water Treat. 21 (2010) 228–237.

[22] F. Atmani, A. Bensmaili, A. Amrane, Methyl orange removal from aqueous solutions by natural and treated skin almonds, Desalin. Water Treat. 22 (2010) 174–181.

[23] R. Srivastava, D.C. Rupainwar, Liquid phase adsorption of indigo carmine and methylene blue on neem bark, Desalin. Water Treat. 24 (2010) 74–84.

[24] E.A. Oliveira, S.F. Montanher, M.C. Rollemberg, Removal of textile dyes by sorption on low-cost sorbents. A case study: Sorption of reactive dyes onto *Luffa cylindrica*, Desalin. Water Treat. 25 (2011) 54–64.

[25] G. McKay, M. Hadi, M.T. Samadi, A.R. Rahmani, M.S. Aminabad, F. Nazemi, Adsorption of reactive dye from aqueous solutions by compost, Desalin. Water Treat. 28 (2011) 164–173.

[26] G.H. Sonawane, V.S. Shrivastava, Removal of hazardous dye from synthetic textile dyeing and printing effluents by *Archis hypogea* L. shell: A low cost agro waste material, Desalin. Water Treat. 29 (2011) 29–38.

[27] Z. Wang, P. Han, Y. Jiao, D. Ma, C. Dou, R. Han, Adsorption of congo red using ethylenediamine modified wheat straw, Desalin. Water Treat. 30 (2011) 195–206.

[28] S. Chowdhury, P. Saha, Pseudo-second-order kinetic models for the sorption of malachite green onto *Tamarindus indica* seeds: Comparison of linear and non-linear methods, Desalin. Water Treat. 30 (2011) 229–236.

[29] U. Farooq, J.A. Kozunski, M.A. Khan, M. Athar, Biosorption of heavy metal ions using wheat based biosorbents, a review of the recent literature, Bioresour. Technol. 101 (2010) 5043–5053.

[30] S. Daneshvar, A.A. Talebi, Y. Fathipour, The wasps associated with seeds and galls of *Rosa canina* in Iran, Adv. Environ. Biol. 3 (2009) 61–68.

[31] M.S. Manis, Biology of insect induced galls, in: J.D. Shorthouse, O. Rohfritsch (Eds.), Introduction to Cecidology, Oxford University Press, New York, NY, 1992, pp. 3–7.

[32] S. Coruh, S. Ercisli, Interactions between galling insects and plant total phenolic contents in *Rosa canina* L. genotypes, Sci. Res. Essays 5 (2010) 1935–1937.

[33] S.M.O. Brito, H.M.C. Andrade, L.F. Soares, R.P. Azevedo, Brazil nut shells as a new biosorbent to remove methylene blue and indigo carmine from aqueous solutions, J. Hazard. Mater. 174 (2010) 84–92.

[34] M.E. Fernandez, G.V. Nunell, P.R. Bonelli, A.L. Cukierman, Effectiveness of *Cupressus sempervirens* cones as biosorbent for the removal of basic dyes from aqueous solutions in batch and dynamic modes, Bioresour. Technol. 101 (2010) 9500–9507.

[35] C. Appel, L.Q. Ma, R.D. Rhue, E. Kennelley, Point of zero charge determination in soils and minerals via traditional methods and detection of electroacoustic mobility, Geoderma 113 (2003) 77–93.

[36] M. Kosmulski, PH dependent surface changing and points of zero charge. IV. Update and new approach, J. Colloid Interface Sci. 337 (2009) 439–444.

[37] R. Gong, S. Zhu, D. Zhang, J. Chen, S. Ni, R. Guan, Adsorption behavior of cationic dyes on citric acid esterifying wheat straw: Kinetic and thermodynamic profile, Desalination 230 (2008) 220–228.

[38] C. Namasivayam, D. Kavitha, Removal of congo red from water by adsorption onto activated carbon prepared from coir pith, an agricultural solid waste, Dyes Pigments 54 (2002) 47–58.

[39] F.E. Bartel, T.L. Thoma, Y. Fu, Thermodynamics of adsorption from solution: IV. Temperature dependence of adsorption, J. Phys. Chem. 55 (1951) 1456–1462.

[40] R. Ahmad, Studies on adsorption of crystal violet dye from aqueous solution onto coniferous pinus bark powder (CPBP), J. Hazard. Mater. 171 (2009) 767–773.

[41] M. Doğan, H. Abak, M. Alkan, Adsorption of methylene blue onto hazelnut shell: Kinetics, mechanism and activation parameters, J. Hazard. Mater. 164 (2009) 172–181.

[42] C.A. BaŞar, Applicability of the various adsorption models of three dyes adsorption onto activated carbon prepared waste apricot, J. Hazard. Mater. B 135 (2006) 232–241.

[43] M.K. Purkait, S. DasGupta, S. De, Adsorption of eosin dye on activated carbon and its surfactant based desorption, J. Environ. Manage. 76 (2005) 135–142.

[44] S.S. Tahir, N. Rauf, Removal of cationic dye from aqueous solutions by adsorption onto bentonite clay, Chemosphere 63 (2006) 1842–1848.

[45] A. Mittal, J. Mittal, A. Malviya, D. Kaur, V.K. Gupta, Decoloration treatment of a hazardous triarylmethane dye, Light Green SF (Yellowish) by waste material adsorbents, J. Colloid Interface Sci. 342 (2010) 518–527.

[46] A.W.M. Ip, J.P. Barford, G. McKay, Reactive Black dye adsorption/desorption onto different adsorbents: Effect of salt, surface chemistry, pore size and surface area, J. Colloid Interface Sci. 337 (2009) 32–38.

[47] V. Jaikumar, V. Ramamurthi, Effects of biosorption parameters kinetic isotherm and thermodynamics for acid green dye biosorption from aqueous solution by brewery waste, Int. J. Chem. 1 (2009) 2–12.

[48] R. Sivaraj, C. Namasivayam, K. Kadirvelu, Orange peel as an adsorbent in the removal of acid violet 17 (acid dye) from aqueous solution, Waste Manage. (Oxford) 21 (2001) 105–110.

[49] R.L. Tseng, F.C. Wu, Inferring favourable adsorption level and the concurrent multistage process with the Freundlich constant, J. Hazard. Mater. 155 (2008) 277–287.

[50] M. Radhika, K. Palanivelu, Adsorptive removal of chlorophenols from aqueous solution by low cost adsorbent, Kinetics and isotherm analysis, J. Hazard. Mater. B 138 (2006) 116–124.